Influence of pump coherence on the dynamic behavior of a laser

J. Pujol and F. Laguarta

Escola Universitaria d'Optica, C/ Colón 1, 08222 Terrassa, Spain

R. Vilaseca

Departament d'Optica, Universitat de Valencia, 46100 Burjassot, Spain

R. Corbalán

Departament de Fisica, Universitat Autònoma de Barcelona, 08193 Bellaterra, Spain

Received August 17, 1987; accepted November 19, 1987

The dynamic behavior of a coherently pumped single-mode unidirectional ring laser with a homogeneously broadened three-level active medium is studied. Our formulation is based on a set of ten real equations of the plane-wave, mean-field Maxwell–Bloch type. The instability domain in the main control parameters space is determined. Our numerical study of these equations for a parameter range of the type explored in the recent experiments by Weiss and Brock [Phys. Rev. Lett. 57, 2804 (1986)] reveals some similarities, but striking differences between our theoretical predictions and their experimental observations are also noted.

Quantum-optical systems like lasers are playing a key role in such an active arena as the study of periodic and chaotic instabilities in nonlinear dynamic systems.[1] In particular, optically pumped lasers (OPL's) operating in the far infrared appear to be[2] promising candidates for solving the long-standing and challenging problem of operating an actual laser in the chaotic regime of the Lorenz–Haken model,[3] and, indeed, some experimental observations[4] qualitatively confirm that prediction. Moreover, single-mode homogeneously broadened OPL's show a wealth of instabilities at reduced pump thresholds in both resonant[4] and off-resonant[5] systems. Most theoretical analysis of laser-light dynamics reported (e.g., see Ref. 1 and references therein) considered an incoherent pumping mechanism and therefore modeled the active laser medium as a two-level system. OPL's are, however, coherently pumped lasers, and theoretical results on their dynamic behavior are scarce, although some progress has been made recently.[6–9]

In this paper we report theoretical studies of the behavior of a coherently pumped single-mode unidirectional ring laser with a homogeneously broadened three-level active medium in which the pumping and lasing transitions share a common upper level (see inset of Fig. 1). We focus on the effects of the coherent optical pumping on the dynamic behavior of a laser, i.e., on three-level effects. Consequently, the study is made here by using the plane-wave approximation, neglecting Doppler broadening, level degeneracy, and propagation effects for both the pump and the generated beams. The aim of these simplifying assumptions is twofold: first, to permit a direct comparison with well-known two-level laser results[3,10] obtained under the same conditions and second, to answer the interesting question of how much of the experimental results can be understood on the basis of the simple model considered here.

We carried out a numerical integration of the OPL model equations and discovered some similarities and also some striking differences between incoherently and coherently pumped lasers. Our analysis also reveals that most of the rich OPL dynamics develop far from steady states and thus suggests that studies based on approximate perturbative solutions likely have only minor relevance to the OPL's actual behavior.

The Maxwell–Bloch type of equations in the rotating-wave approximation for our system can be shown to be[6]

$$
\begin{aligned}
\dot{\rho}_{00} &= \gamma_0(\rho_{00}{}^0 - \rho_{00}) - 2\alpha\,\mathrm{Im}(\rho_{01}) - 2\beta\,\mathrm{Im}(\rho_{02}),\\
\dot{\rho}_{11} &= \gamma_1(\rho_{11}{}^0 - \rho_{11}) + 2\alpha\,\mathrm{Im}(\rho_{01}),\\
\dot{\rho}_{22} &= \gamma_2(\rho_{22}{}^0 - \rho_{22}) + 2\beta\,\mathrm{Im}(\rho_{02}),\\
\dot{\rho}_{01} &= -\gamma_{01}\rho_{01} + i[\Delta_1{}^c - G\,\mathrm{Re}(\rho_{01})/2\alpha]\rho_{01}\\
&\quad - i\beta\rho_{21} + i\alpha(\rho_{00} - \rho_{11}),\\
\dot{\rho}_{02} &= -\gamma_{02}\rho_{02} - i\Delta_2\rho_{02} - i\alpha\rho_{12} + i\beta(\rho_{00} - \rho_{22}),\\
\dot{\rho}_{12} &= -\gamma_{12}\rho_{12} - i[(\Delta_1{}^c - \Delta_2)\\
&\quad - G\,\mathrm{Re}(\rho_{01})/2\alpha]\rho_{12} - i\alpha\rho_{02} - i\beta\rho_{10},\\
\dot{\alpha} &= G\,\mathrm{Im}(\rho_{01})/2 - \gamma_c\alpha/2.
\end{aligned}
\tag{1}
$$

Here ρ_{ij} $(i, j = 0, 1, 2)$ are slowly varying envelopes of density-matrix elements normalized to the density N^0 of molecules in the three-level system, and $\rho_{ii}{}^0$ are the zero-field populations; γ_i, γ_{ij} $(i, j = 0, 1, 2)$, and γ_c are the population, coherence, and cavity decay rates, respectively; $\Delta_1{}^c = w_c - w_{01}$ and $\Delta_2 = w_2 - w_{02}$ are detunings, where w_c and w_2 are the cavity and pump field frequencies, respectively; and w_{01} and w_{02} are the amplifying and absorbing transition frequencies.

0740-3224/88/051004-07$02.00

$2\alpha(t)$ and 2β are real Rabi frequencies that characterize the interaction of a molecule with the generated and pump fields, where β is supposed to be constant and $\alpha(t)$ gives a measure of the generated field amplitude at each instant t. $G = w_{01}\mu_{01}^2 N^0/\epsilon_0\hbar$, where μ_{01} is the transition dipole moment, is a parameter that accounts for the strength of the molecule-generated field coupling and for the density of the molecules. Because the ρ_{ij} $(i \neq j)$ coherences are complex functions, the basic equations of motion [Eqs. (1)] constitute a set of ten real first-order differential equations. Finally, we note that the generated frequency w_1 can be calculated by using the following well-known frequency-determining equation:

$$w_1(t) - w_{01} = \Delta_1(t) = \Delta_1^c - G\,\mathrm{Re}(\rho_{01})(t)/2\alpha.$$

Some predictions of this model were presented recently,[6-9] but owing to the versatility of the three-level system there remain many unexplored questions. In some cases (e.g., by adiabatic elimination of fast variables) the dynamics of OPL reduce to a system with less than ten degrees of freedom. Thus Dupertuis *et al.*[6] have listed six conditions that are required to reduce the dynamics of the present model to that of the three-equation Lorenz–Haken model,[3] and Lawandy and Ryan[9] worked out a four-equation version of the OPL model that predicts instabilities at pump intensities as low as 1.6 times above threshold. Mehendale and Harrison[7] investigated the case with $\Delta_1^c = \Delta_2 = \Delta_1 = 0$; $\gamma_i = \gamma_{ij} = \gamma$ $(i, j = 0, 1, 2)$, and $\gamma_c > \gamma$, for which, surprisingly, only regular self-pulsing instabilities were found.

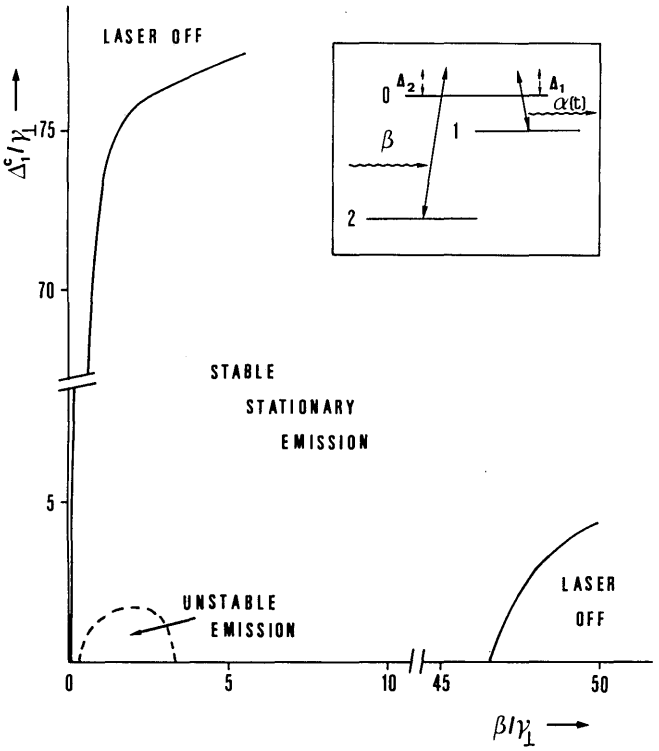

Fig. 1. Phase diagram of an optically pumped laser in the (β, Δ_1^c) plane as predicted by the LSA of the stationary solutions of Eqs. (1). The continuous curves correspond to the first laser threshold, and the dashed line corresponds to the second laser threshold within the LSA (onset of a supercritical Hopf bifurcation). The parameters used in the calculations are given in the text. The inset represents schematically the three-level system considered in this paper.

Instead of imposing simplifying mathematical conditions on the operating parameters, our numerical study of the model equations was made for a parameter range of the type explored in the experiments of Weiss and Brock,[4] who, to our knowledge, reported the first observation of Lorenz-type chaos in the 81.5-μm emission from a $^{14}NH_3$ laser pumped with the $P(13)$ line of the N_2O laser. We considered the cavity detuning Δ_1^c and the pump field amplitude β to be the main control parameters. For the remaining parameters the following values were adopted,[11] referring to a 10-Pa $^{14}NH_3$ pressure: $\gamma_{01} \equiv \gamma_\perp = 6.8 \times 10^6\ \mathrm{sec}^{-1}$; $\gamma_0 = \gamma_1 \equiv \gamma_\parallel = 0.28\gamma_\perp$; $\gamma_2 = \gamma_{12} = \gamma_{02} = 0.95\,\gamma_\perp$; $\gamma_c = 2.85\,\gamma_\perp$; $\Delta_2 = 0$; $\rho_{11}^0 = \rho_{00}^0 = 0$; and $N^0 = 1.07 \times 10^{19}\ \mathrm{m}^{-3}$. To adhere to the standard notation used in models based on two-level atoms, we introduced the longitudinal and transverse decay rates, $\gamma_\parallel$ and $\gamma_\perp$, respectively, associated with the 0–1 lasing transition. The bad-cavity condition is fulfilled, and the coincidence in order of magnitude between all the relaxation rates prevents any adiabatic elimination of variables. Thus the results shown below correspond to the behavior of an OPL in conditions *a priori* different from those required[6] to observe a Lorenz instability.

The fixed points of Eqs. (1) are the emissionless state $\alpha = 0$ and the stationary lasing state with $\alpha \neq 0$. As a first step, we determined, for different values of the control parameters (β, Δ_1^c), the corresponding steady lasing states, which turned out to be unique always, except for an unphysical indetermination in the α sign[12] (i.e., no multistability was found). A linear stability analysis (LSA) allowed us to determine the domain in the parameter plane (β, Δ_1^c) at which the stationary solutions become unstable. These findings are summarized in Fig. 1. Within the LSA, the OPL instability appears with a Hopf bifurcation at the boundaries shown by the dashed line in Fig. 1. Even if the laser instability appears only in a rather small domain of the (β, Δ_1^c) parameter plane, this domain is within easy experimental reach because reaching this domain requires a moderate pump power and a resonant or near-resonant cavity tuning. In fact, β values much larger than those corresponding to the instability domain are at present difficult to obtain with unfocused pump beams.

Next, to localize and characterize the different attractors in the phase space of our OPL system and to study their evolution under control parameter changes (i.e., phase or bifurcation diagram), we solved the dynamic equations (1) by using a seventh–eighth-order Runge–Kutta routine, and we computed intensity-power spectra of the output field by using a fast-Fourier-transform routine. This study is limited at present to the resonant case $(\Delta_1^c = 0)$ and to a small range of pump powers that are close to the LSA instability threshold, which is at present the most interesting case because it corresponds to the experiments performed thus far.[4]

When we studied the long-time behavior of the OPL, we found two attractors in its phase space. Figure 2 displays projections in the $(\alpha/\gamma_\perp, \mathrm{Im}\ \rho_{01})$ plane of these two attractors for different values of the pump field amplitude $\beta/\gamma_\perp$. As expected from the LSA, the first attractor, represented by the dashed line in Fig. 2, appears at the first laser threshold $(\beta_{th}/\gamma_\perp = 0.0067)$ as a fixed point (stable focus) associated with the steady lasing state and remains so up to $\beta/\gamma_\perp = 0.34$. At this point the system undergoes a supercritical Hopf bifurcation to a stable small-amplitude limit cycle, which abruptly disappears at $\beta/\gamma_\perp = 0.35$.

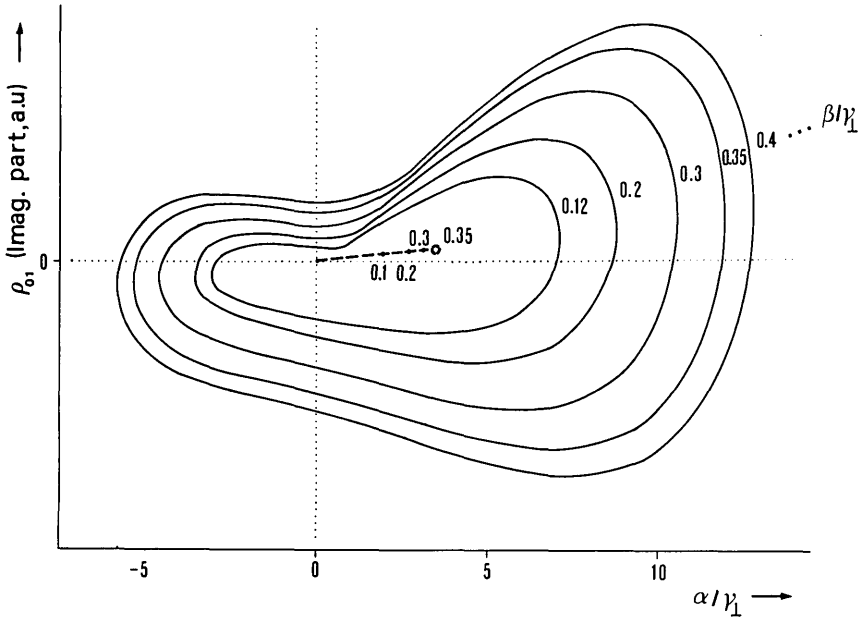

Fig. 2. Phase space portraits of the two attractors for the dynamic variables Im ρ_{01} and $\alpha/\gamma_\perp$ for increasing values of the pump field amplitude $\beta/\gamma_\perp$: dashed curve, first attractor (successive positions of the stable fixed point); dashed circumference, limit cycle; solid curves, outermost limits of the second attractor (area surrounded or covered by the attracted trajectories). The dynamic behaviors associated with each attractor are reported in Fig. 3.

The discovery of a second much more physically relevant attractor, whose outermost limits are represented by the continuous lines of Fig. 2, is our main finding. This attractor is present at first at $\beta/\gamma_\perp = 0.12$, where it already covers a large region of phase space that continuously expands for increasing β. The basin of attraction for this attractor, which is much larger than the basin for the previous attractor, includes the unstable fixed point $\alpha = 0$ with abrupt switching of the gain. Therefore, the laser instability appears now as a hard-mode excitation at the pump threshold[13] $\beta_{ins}/\gamma_\perp = 0.12$, a value that is much less than that required for the Hopf bifurcation at $\beta/\gamma_\perp = 0.34$.

Figure 3 represents schematically the dynamic behavior associated with each attractor as a function of pump field amplitude. When $\beta/\gamma_\perp$ is increased, the second attractor (lower strip in Fig. 3) appears abruptly and with a dominance of chaos, and after two relatively large period-3 and period-6 windows of regular pulsing in the chaotic range, the OPL follows a regular pulsing route of period-10, period-8, period-4 out of chaos. A period-2 pulsing was not found, and for larger values of $\beta/\gamma_\perp$ the pulsing period increased again. As noted above, the attractor inverse of the present attractor, obtained by making the transformation (α; ρ_{01}; ρ_{12}) $\rightarrow$ ($-\alpha$; $-\rho_{01}$; $-\rho_{12}$), also exists. However, for the parameter range explored here both attractors appear unconnected. For this reason, the motion of the OPL system takes place around only one $\alpha \neq 0$ center, as can be seen in Fig. 2. This dynamic feature of the OPL is in fair contrast with the behavior of the chaotic Lorenz system, for which the trajectory in the field-polarization plane appears to switch randomly from the neighborhood of one of the (unstable) fixed points to the neighborhood of the other fixed point.[1] (Compare Fig. 2 also with Fig. 6 below, which shows the second attractor in the chaotic range when some of the conditions of Ref. 6 are approximately satisfied.)

If we examine the time evolution of the intensity $\alpha^2(t)$, then all the P^n limit cycles referred to in Fig. 3, which are asymmetric in the (α, Im ρ_{01}) plane, will appear in the emitted intensity as a periodic self-pulsing of period $2nP$.

The (Re ρ_{12}, α, Im ρ_{01}) three-dimensional picture of the second attractor, the corresponding time evolution at the (α, Im ρ_{01}) projection, and the power spectrum of the α^2 emitted intensity are given in Fig. 4 for the chaotic range and in Fig. 5 for the period-4 pulsing range. For brevity and to facilitate the comparison of the present attractor with the Lorenz attractor, which is usually plotted in the field-polarization plane (see, e.g., Ackerhalt *et al.*[1]), we chose to display only the α, Im ρ_{01}, and Re ρ_{12} variables of the ten possible dynamic variables. We have verified, however, that all the remaining variables show the same kind of dynamic behavior. Figure 5a also shows the transient temporal evolution in order to show the characteristic outward spiraling around the unstable fixed point at (3.57, 3.88 $\times$ 10^{-4}). This spiraling

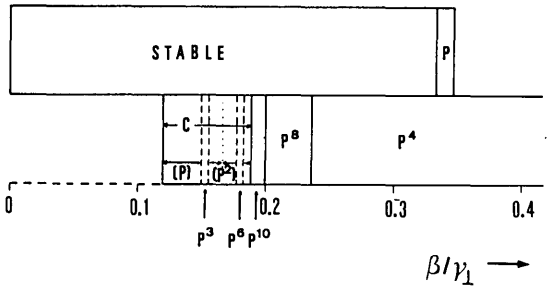

Fig. 3. Bifurcation diagram of the centrally tuned optically pumped laser. The upper strip corresponds to the first attractor, and the lower strip corresponds to the second attractor (see Fig. 1): P^n's, periodic pulsing of periods nP; C, chaotic emission; P^3 and P^6 are periodic windows within the chaotic domain. Within the chaotic domain, the sign (P) at the left-hand side of the vertical dotted line and the sign (P^2) at the right-hand side indicate that the respective periodic pulsings are still apparent in spite of their strong modulation by the intense and broad bandwidth chaos.

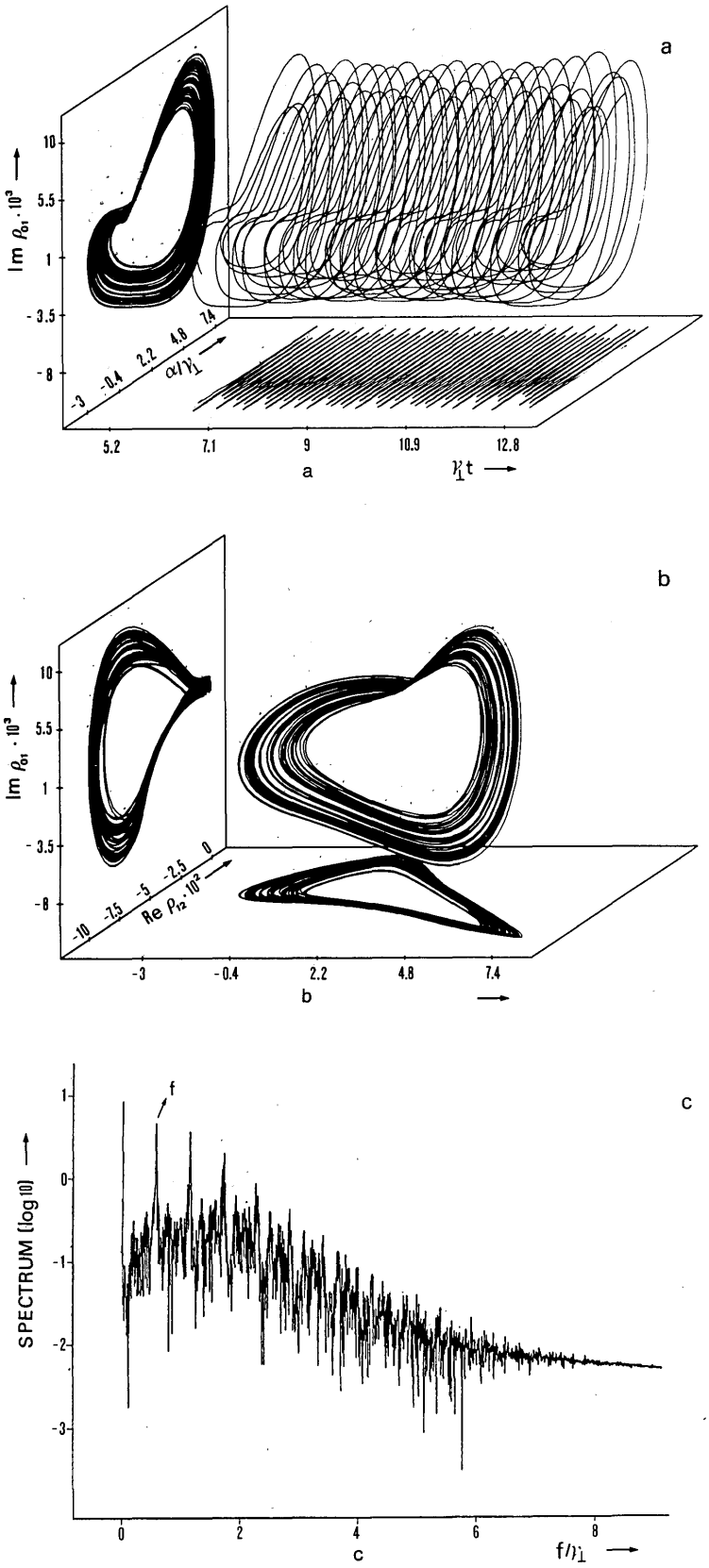

Fig. 4. The second attractor (see Figs. 2 and 3) at $\beta/\gamma_\perp = 0.14$: a, long-term time evolution of the (α, Im ρ_{01}) projection; b, (Re ρ_{12}, α, Im ρ_{01}) projection of the attractor (ρ_{12} coherence gets values larger than ρ_{01} coherence); c, power spectrum of $\alpha^2(t)$ on a semilogarithmic scale. In c note the broadband character of the spectrum, which is considered a signature of chaos. The spectral line at $f/\gamma_\perp = 0.55$ and its harmonics indicate that even in the chaotic range the pulsing frequency is quite well defined. This frequency f, indicated by an arrow in the figure, corresponds to the inverse of the time interval separating two consecutive positive peaks in the $\alpha(t)$ signal. The corresponding frequency for the intensity signal $\alpha^2(t)$ is $2f$.

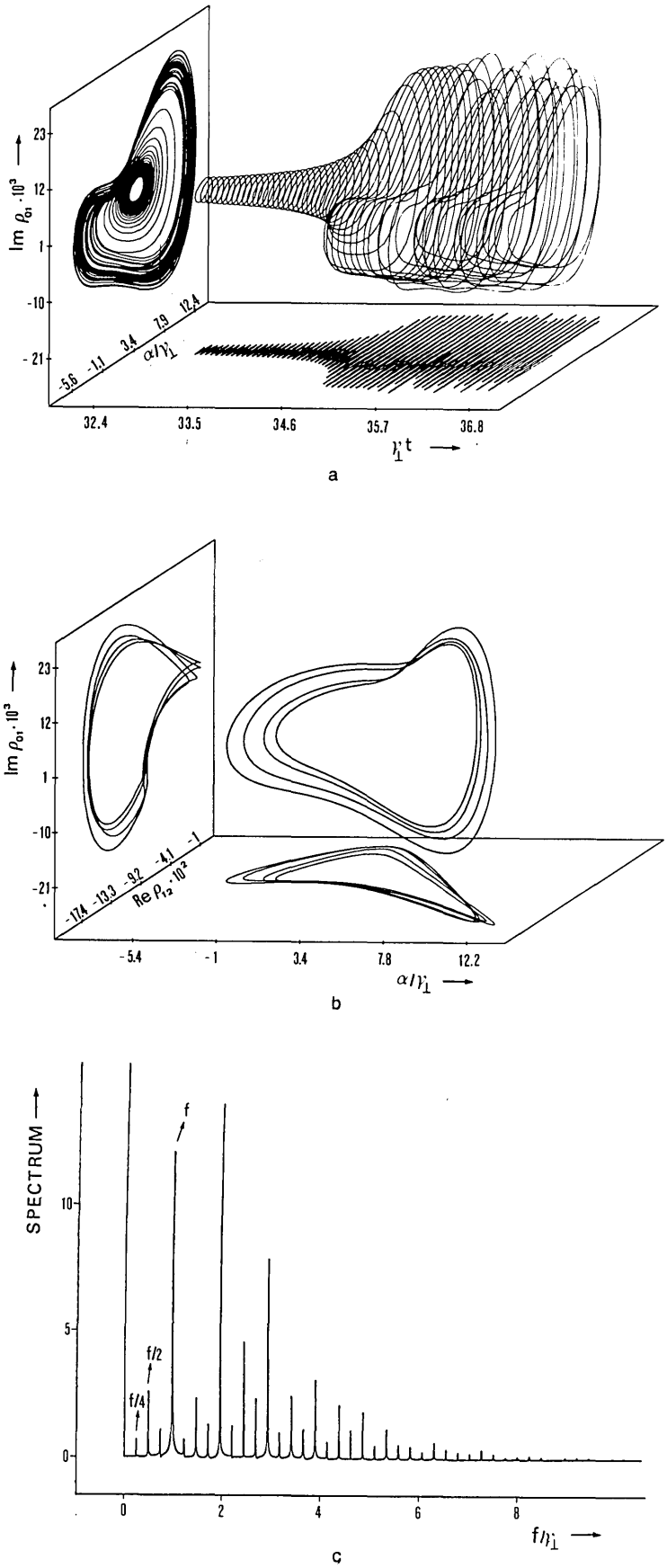

Fig. 5. The second attractor (see Figs. 2 and 3) at $\beta/\gamma_\perp = 0.36$: a, final portion of the transient time evolution of the (α, Im ρ_{01}) projection; b, (Re ρ_{12}, α, Im ρ_{01}) projection of the trajectory after transients have died out; c, power spectrum of $\alpha^2(t)$. Contrary to Fig. 4c, the vertical scale here is linear. The frequency f, marked with an arrow, is defined in the caption to Fig. 4.

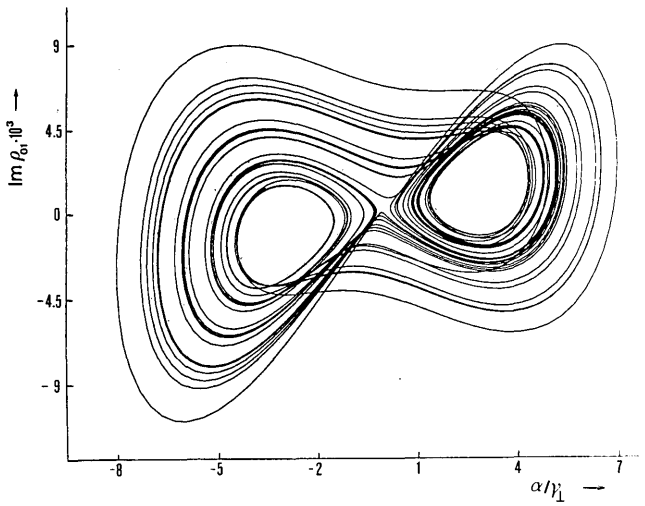

Fig. 6. (α, Im ρ_{01}) projection of the second attractor for $\gamma_{12}/\gamma_\perp$ = 6.51. Other parameters are as in Fig. 4.

evolves slowly, owing to the system memory of the first attractor's limit cycle, which has just become unstable at $\beta/\gamma_\perp = 0.35$. Figures 4a and 4c also show that even in the chaotic range the basic pulsing frequency is quite well defined. The broadband power spectrum characteristic of chaotic pulsing appears superimposed upon the basic pulsing frequency $f/\gamma_\perp = 0.55$ and its harmonics (Fig. 4c). The difference between this spectrum and the spectrum corresponding to period-4 pulsing is striking. Figure 5c shows a collection of well-defined peaks corresponding to the fundamental frequency $f/\gamma_\perp = 0.97$, the subharmonics $f/2$ and $f/4$, and their harmonics. Moreover, we can appreciate in Figs. 4b and 5b that the two-quantum coherence ρ_{12} has values even larger than the ρ_{01} coherence, thus indicating a strong coherent interaction between the pump and the generated waves. In fact, this coherent interaction depends on the existence of the ρ_{12} coherence and can be eliminated if a relaxation mechanism is introduced to destroy specifically the two-quantum coherence. This effect is shown in Fig. 6, in which the (α, Im ρ_{01}) projection of the second attractor is shown for an artificially increased rate $\gamma_{12} = 6.51\gamma_\perp$ and other parameters, as in Fig. 4. We can observe now an OPL dynamic behavior similar to that of the Lorenz model. A detailed study to show dynamically how the second attractor found here approaches the Lorenz attractor when the conditions of Ref. 6 become progressively satisfied is left for a subsequent paper.

In conclusion, we have investigated numerically a model for a resonantly tuned OPL for a parameter range of the type explored in the experiments of Weiss and Brock.[4] This model predicts that for pump powers high above threshold ($\beta_{ins}^2/\beta_{thr}^2 \approx 75$), a rich and varied dynamic behavior develops far from the fixed points of the OPL system and thus cannot be obtained from descriptions based on perturbative formulations. Our results reproduced qualitatively some signatures of the Lorenz model observed in the experiment,[4] such as an abrupt transition from continuous emission to chaotic emission. Moreover, Fig. 3 shows coexistence between the steady-state attractor and the chaotic attractor, which could be at the origin of the observed[4] hysteresis between the chaotic state and the cw state with respect to the pump power. We believe, however, that this agreement between our results and the corresponding predictions of the Lorenz model is somewhat accidental because our conditions were different than those needed to make our OPL model equivalent to the Lorenz model. The chaotic laser pulses appeared also in our numerical simulations with a fairly well-defined pulsing frequency but, in contrast to the experiment, did not show the characteristic pulsing of the Lorenz system. This difference can be traced to the spiraling of our system around only one center; spiraling around two centers is characteristic of the Lorenz system [compare Fig. 4a with Fig. 4(a) of Ref. 4]. We were not able to obtain the period-3 and period-5 windows of regular motion in the chaotic range observed in the experiment.[4] Moreover, our model predicts dynamic behaviors such as the sequence period-10, period-8, period-4 of regular pulsing that is not present in the Lorenz model. Therefore this sequence can be considered a signature of the OPL. The extension of this study to a wider parameter range, including the detuned ($\Delta_1^c \neq 0$) case, is currently under way and will be the subject of a future publication.

ACKNOWLEDGMENTS

We wish to thank C. O. Weiss for sending us his results prior to publication and for discussions related to his experiment. We also are grateful to E. Arimondo and J. R. Tredicce for useful discussions and criticism of the manuscript. The assistance of C. Simó, who made available a general-purpose simulation package and gave us some insight into dynamic systems, is especially appreciated.

REFERENCES AND NOTES

1. To get a certain feeling of the vitality of the field of optical chaos see, for instance, the feature issue on Instabilities in Active Optical Media, J. Opt. Soc. Am. B **2**, 1–272 (1985); R. W. Boyd, M. G. Raymer, and L. M. Narducci, eds., *Optical Instabilities* (Cambridge U. Press, Cambridge, 1986); J. R. Ackerhalt, P. W. Milonni, and M. L. Shih, "Chaos in quantum optics," Phys. Rep. **128**, 205–300 (1985); R. G. Harrison and D. J. Biswas, "Chaos in light," Nature **131**, 394–401 (1986); in *Technical Digest of the International Workshop on Instabilities, Dynamics, and Chaos in Nonlinear Optical Systems* (ETS Editrice, Pisa, 1987).
2. C. O. Weiss and W. Klische, "On observability of Lorenz instabilities in lasers," Opt. Commun. **51**, 47–48 (1984).
3. H. Haken, "Analogy between higher instabilities in fluids and lasers," Phys. Lett. A **53**, 77–78 (1975).
4. C. O. Weiss and J. Brock, "Evidence for Lorenz-type chaos in a laser," Phys. Rev. Lett. **57**, 2804–2806 (1986).
5. R. G. Harrison and D. J. Biswas, "Demonstration of self-pulsing instability and transitions to chaos in single-mode and multimode homogeneously broadened Raman laser," Phys. Rev. Lett. **55**, 63–66 (1985).
6. M. A. Dupertuis, R. R. E. Salomaa, and M. R. Siegrist, "The conditions for Lorenz chaos in an optically pumped far-infrared laser," Opt. Commun. **57**, 410–414 (1986).
7. S. C. Mehendale and R. G. Harrison, "Spontaneous mode splitting in optically pumped molecular laser due to the ac Stark effect," Phys. Rev. A **34**, 1613–1616 (1986); "Theoretical analysis of instabilities in optically pumped molecular lasers," Opt. Commun. **60**, 257–260 (1986).
8. J. Pujol, R. Vilaseca, R. Corbalán, and F. Laguarta," Instabilities in optically pumped infrared lasers," Int. J. Infrared Millimeter Waves **8**, 299–305 (1987).
9. N. M. Lawandy and J. C. Ryan, "Instabilities in a coherently pumped laser," in *Digest of XV International Quantum Elec-*

tronics Conference (Optical Society of America, Washington, D.C., 1987), pp. 140–141.
10. H. Zeghlanche and P. Mandel, "Influence of detuning on the properties of laser equations," J. Opt. Soc. Am. B **2**, 18–22 (1985).
11. N. M. Lawandy and D. V. Plant, "On the experimental accessibility of the self-pulsing regime of the Lorenz model for single-mode homogeneously broadened lasers," Opt. Commun. **59**, 55–58 (1986).
12. It can be shown that for any given solution of Eqs. (1) another solution exists that only differs in the signs of the variables α, ρ_{01}, and ρ_{12}. These two solutions correspond to the same stationary intensity α^2.
13. The positions of the first and second laser threshold depend sensitively on the initial populations. To get physically meaningful values, we need to take into account the small initial population existing in levels 0 and 1 ($\rho_{00}{}^0:\rho_{11}{}^0:\rho_{22}{}^0$ = 0.0114:0.0183:0.9703), and we obtain: $\beta_{thr}/\gamma_\perp = 0.030$ and $\beta_{ins}/\gamma_\perp = 0.26$. These results imply a theoretical ratio $\beta_{ins}{}^2/\beta_{thr}{}^2 \approx 75$, about five times higher than the experimental value.[4] This discrepancy between the predicted and measured laser-threshold ratios is not too surprising in view of the simplifications of our model. In particular, the Doppler broadening, which we have ignored, is known to lower the instability threshold with respect to the homogeneous-broadening case.